Eu^{3+} parity-forbidden intra-f-shell crystal-field transition $^5D_0 \rightarrow {}^7F_2$, the short component is not attributed to Eu^{3+}, but to the very weak intrinsic background luminescence from the TiO_2 defect centers. Here it should be emphasized that no significant decrease in the PL lifetimes is observed when the Eu^{3+} content is increased. This indicates that even at europium concentrations as high as 8 mol% no quenching of the Eu^{3+} $^5D_0 \rightarrow {}^7F_2$ luminescence is present.

In summary, for the first time, a cubic mesostructured matrix of titania with a three-dimensional array of embedded anatase nanocrystals has been doped with high concentrations of europium ions. The semiconducting anatase nanocrystallites sensitize the europium activator, which leads to an energy transfer system that produces a bright red, near-monochromatic luminescence. This work represents an interesting optical application of an all-inorganic mesoporous material. These have, because of their robust self-assembled framework, high surface area, simple processability, and air and moisture stability, potential to be incorporated into optical devices. The ability of the cubic mesostructured titania films to retain their structure and properties after the addition of a large amount of dopants opens the field to three-dimensionally ordered multicomposite materials for new electrical, magnetic, and optical applications.

Experimental Section

A typical trivalent europium ion doped, red photoluminescent film was prepared by dissolving $EuCl_3 \cdot 6H_2O$ (0.51 g) and Pluronic P123 (1 g) in absolute ethanol (12 g). This solution was added to a solution containing concentrated hydrochloric acid (2.7 mL) and titanium(IV) ethoxide (3.88 mL). After the solution had been aged, films were deposited on glass or quartz substrates by dip-coating at a rate of 1 mm s^{-1}. The films were heat-treated for 4 h at 400 °C.

UV/Vis absorption spectra of these films were measured by using a Shimadzu UV-1610 recording spectrometer. The PL emission and excitation spectra were recorded with a Cary Eclipse PL spectrometer. For the PL lifetime measurements the films were excited with the 337 nm line of a pulsed (1 ns pulse width) nitrogen laser. The emission was dispersed by a monochromator and analyzed by using a digital oscilloscope.

Received: November 29, 2001 [Z18299]

[1] a) P. Yang, D. Zhao, D. I. Margolese, B. F. Chmelka, G. D. Stucky, *Nature* **1998**, *396*, 152–155; b) J. Y. Ying, C. P. Mehnert, M. S. Wong, *Angew. Chem.* **1999**, *111*, 58–82; *Angew. Chem. Int. Ed.* **1999**, *38*, 56–77; c) D. M. Antonelli, *Microporous Mesoporous Mater.* **1999**, *30*, 315–319; d) S. Cabrera, J. El Haskouri, A. Beltrán-Porter, D. Beltrán-Porter, M. D. Marcos, P. Amorós, *Solid State Sci.* **2000**, *2*, 513–518; e) Y. Wang, X. Tang, L. Yin, W. Huang, Y. Rosenfeld Hacohen, A. Gedanken, *Adv. Mater.* **2000**, *12*, 1183–1186.

[2] a) P. Yang, D. Zhao, D. I. Margolese, B. F. Chmelka, G. D. Stucky, *Chem. Mater.* **1999**, *11*, 2813–2816; b) P. Alberius-Henning, K. L. Frindell, R. C. Hayward, E. J. Kramer, B. F. Chmelka, G. D. Stucky, *Chem. Mater.* submitted.

[3] a) D. Grosso, G. J. de A. A. Soler-Illia, F. Babonneau, C. Sanchez, P.-A. Albouy, A. Brunet-Bruneau, A. R. Balkenende, *Adv. Mater.* **2001**, *13*, 1085–1090; b) Y. K. Hwang, K.-C. Lee, Y.-U. Kwon, *Chem. Commun.* **2001**, 1738–1739.

[4] A. Conde-Gallardo, M. García-Rocha, I. Hernández-Calderón, R. Palomino-Merino, *Appl. Phys. Lett.* **2001**, *78*, 3436–3438.

[5] a) S. Hüfner, *Optical Spectra of Transparent Rare Earth Compounds*, Academic Press, New York, **1978**; b) J. Ballato, J. S. Lewis III, P. Holloway, *MRS Bull.* **1999**, *24*, 51–56; c) R. G. Denning, *J. Mater. Chem.* **2001**, *11*, 19–28.

[6] *CRC Handbook of Chemistry and Physics*, 74th ed. (Ed.: D. R. Lide), CRC, Boca Raton, **1993–1994**.

[7] M. R. Hoffmann, S. T. Martin, W. Choi, D. W. Bahnemann, *Chem. Rev.* **1995**, *95*, 69–96.

[8] G. Pucker, K. Gatterer, H. P. Fritzer, M. Bettinelli, M. Ferrari, *Phys. Rev. B* **1996**, *53*, 6225–6234.

[9] Y. Liu, R. O. Claus, *J. Am. Chem. Soc.* **1997**, *119*, 5273–5274.

Multiple Emissions from 1,3-Diphenyl-5-pyrenyl-2-pyrazoline Nanoparticles: Evolution from Molecular to Nanoscale to Bulk Materials**

Hongbing Fu, B. H. Loo, Debao Xiao, Ruiming Xie, Xuehai Ji, Jiannian Yao,* Baowen Zhang, and Lianqi Zhang

The size dependence of organic crystals has not been as well investigated as that of inorganic crystals. The strong effects of confinement on electron–hole pairs in all three dimensions result in the size-tunable optoelectronic properties of semiconductor quantum dots,[1, 2] but are not expected in organic molecular crystals (OMCs), because of the small radius of the Frenkel exciton.[3] The primary difference between inorganic and organic semiconductors is the bandwidth, or the degree of orbital overlap. In the case of OMCs, the electronic and optical properties are fundamentally different from those of inorganic semiconductors, because of weak van der Waals intermolecular forces.[3, 4] To date, the search for ways of controlling size, shape, and hence the properties of OMCs is still a challenge[5–9], and an important aspect in the development of nanoscience.

Size effects may also be significant in OMCs.[5, 6] In our previous work, the size dependence of the optical properties of nanoparticles consisting of 1-phenyl-3-((*p*-dimethylamino)-styryl)-5-((*p*-dimethylamino)phenyl)-2-pyrazoline (PDDP) was shown to originate from charge-transfer (CT) exciton formation, with increasing nanoparticle size.[10] Herein, the newly synthesized 1,3-diphenyl-5-pyrenyl-2-pyrazoline (DPP) is used as a model compound, in the light-emitting layer of an electroluminescent device, because of its strong, blue

[*] Prof. J. Yao, Dr. H. Fu, D. Xiao, R. Xie, X. Ji
Center for Molecular Science, Institute of Chemistry
Chinese Academy of Sciences
Beijing 100080 (P.R. China)
Fax: (+86) 10-64879375
E-mail: jnyao@ipc.ac.cn
Prof. B. H. Loo
Department of Chemistry
University of Alabama, Huntsville, AL 35899 (USA)
Prof. B. Zhang, Dr. L. Zhang
Technical Insititute of Physics and Chemistry
Chinese Academy of Sciences, Beijing 100101 (P.R. China)

[**] This research was supported in part by the National Natural Foundation of China, the National Research Fund for Fundamental Key Projects No. 973 (G19990330) and the Chinese Academy of Sciences.

  1433-7851/02/4106-0962 $ 17.50+.50/0

pyrazoline fluorescence.[11] DPP contains two chromophores, the pyrene and pyrazoline groups. The pyrene ring at the 5-position is almost perpendicular to the parent pyrazoline ring because of the large volume of the pyrene group, and thus their conjugated systems are separate from each other. It is interesting that a dilute solution of DPP in acetonitrile or tetrahydrofuran exhibits only the emission characteristics of the pyrene chromophore. In contrast, in the electroluminescent device, DPP shows only the emission characteristics of the pyrazoline chromophore.[11] We found that DPP nanoparticles exhibit multiple emissions from both pyrene and pyrazoline groups and from a CT complex between pyrene and pyrazoline. The emission color of DPP nanoparticles is tunable between near-UV to green, by alteration of both the excitation wavelength and the nanoparticle size. For organic materials, luminescence applications and the multiple emissions of DPP nanoparticles are likely to be important in tailoring the properties of organic molecules to the resulting structures at nanoscale. In addition, the evolution of pyrene and pyrazoline emission in DPP nanoparticles caused by molecular aggregation and surface effects improves our understanding of the fundamental processes connecting OMCs.

DPP nanoparticless were prepared using a simple reprecipitation method.[5, 10] In this process, a molecularly disperse solution of DPP in a water-miscible solvent, acetonitrile, is mixed vigorously with an aqueous phase. Mixing the solvent and water phases changes the character of the solvent and induces the nucleation and growth of DPP nanoparticles. Figure 1 presents some field-emission scanning-electron

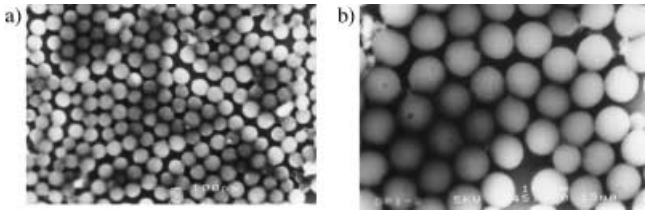

Figure 1. FESEM photographs of DPP nanoparticles with different sizes. a) 120 nm; b) 310 nm.

microscopy (FESEM) photographs of the DPP nanoparticles, in which the average nanoparticle sizes are 120 and 310 nm, respectively. These values agree roughly with those determined by dynamic light scattering (DLS), in which the polydispersity was less than 10%.[12] It can be seen from Figure 1 that the narrow size distribution of DPP nanoparticles caused them to self-assemble into a two-dimensional array, in a way similar to that observed for many other colloidal particles.[13] Measurements of the surface potential of these nanoparticles showed that they are negatively charged, and that the ξ-potential retained a value of about -32 mV with varying nanoparticle size.

Figure 2 displays the UV/Vis absorption spectra of DPP nanoparticles of different sizes, dispersed in water. Compared with the absorption spectrum of a 1,3-diphenyl-2-pyrazoline (DP) solution in ethanol, the spectrum of the dilute DPP in acetonitrile solution is apparently a combination of the

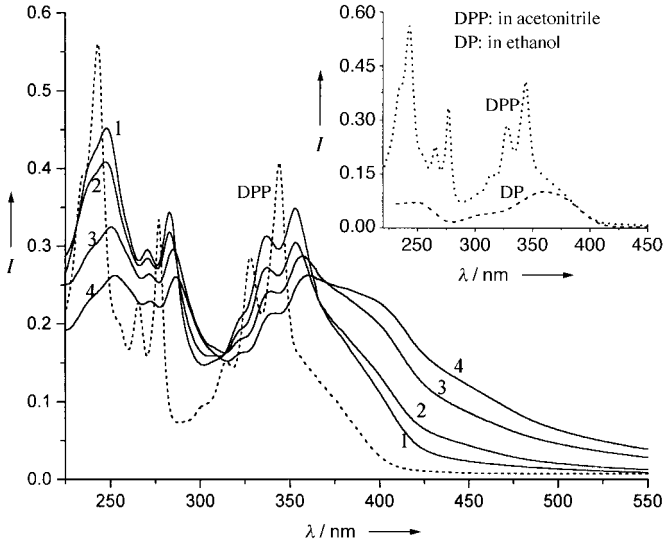

Figure 2. The UV/Vis spectrum of DPP nanoparticles of 1) NP1, 65 nm; 2) NP2, 120 nm; 3) NP3, 180 nm, and 4) NP4, 310 nm in aqueous dispersions. Inset: DPP in acetonitrile solution with a concentration of 1.0×10^{-5} mol L^{-1}, DP in ethanol solution with a concentration of 8.0×10^{-6} mol L^{-1}. I = relative intensity.

spectra of the pyrene and pyrazoline groups (inset in Figure 2). On going from spectrum 1 to 4, with increasing nanoparticle size, the absorption features of the pyrazoline chromophore become gradually more prominent in the region from 370 nm to 420 nm, while the absorption bands of pyrene shift to longer wavelengths. Moreover, a new feature gradually appears at about 450 nm.

The emission spectrum of the DPP in acetonitrile solution (Figure 3A) demonstrates the characteristics of the pyrene group monomer emission bands at 380–410 nm, and a structureless band at 520 nm assigned to a pyrene excimer.[11] In contrast, the spectrum of DPP bulk crystals shows an emission band centered at 445 nm (see Figure 3F). The shape of the emission of the DPP bulk crystals is similar to that of DP bulk crystals. There are significant differences between the fluorescence features of nanoparticles and those of monomers and bulk crystals. Figure 3D (nanoparticle NP3) is typical of the fluorescence features of nanoparticles. The nanoparticle emission (black line) divides into three parts at 385, 465, and 570 nm. The red, yellow, and blue lines are the excitation spectra obtained by monitoring the emissions at 385, 465, and 570 nm, respectively. We found that the intensity of the different emission parts at different excitation wavelength, λ_{ex}, is proportional to the intensity at λ_{ex} in their corresponding excitation spectra. For example, when λ_{ex} is fixed at 290 nm, the first part of the emission vanishes, while the second and third parts are still observed and the second part becomes the strongest. The multiple emissions have different individual optical channels, and can be tuned easily by the selection of λ_{ex}.

Figure 4 shows the proposed emission transitions for DPP in monomers, nanoparticles, and bulk crystals, based on the above spectroscopic study as well as on the fluorescence decay times given in Table 1. For DPP, the first part of the nanoparticle emission at 380–410 nm apparently arises from the pyrene group. Through comparison with the emission

  1433-7851/02/4106-0963 $ 17.50+.50/0

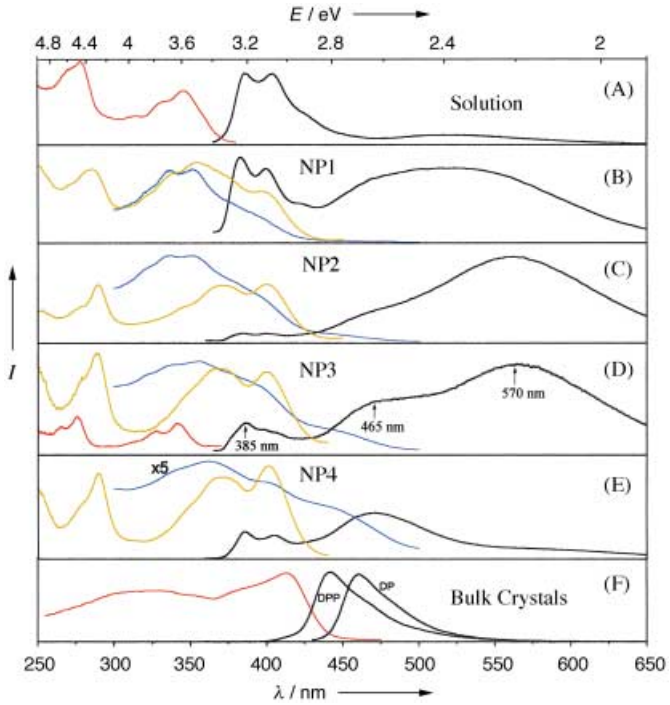

Figure 3. The fluorescence excitation and emission spectra of A) DPP in acetonitrile with a concentration of 1.0×10^{-5} mol L^{-1}; and nanoparticles of B) NP1, C) NP2, D) NP3 and E) NP4; F) DPP and DP bulk crystals. The colored lines are the excitation spectra obtained by monitoring the emission at 385 (red), 465 (yellow), and 570 nm (blue), except for the red line in E, which was obtained by monitoring the emission at 445 nm. Black lines are emission spectra obtained by excitation at 345 nm. I = relative intensity.

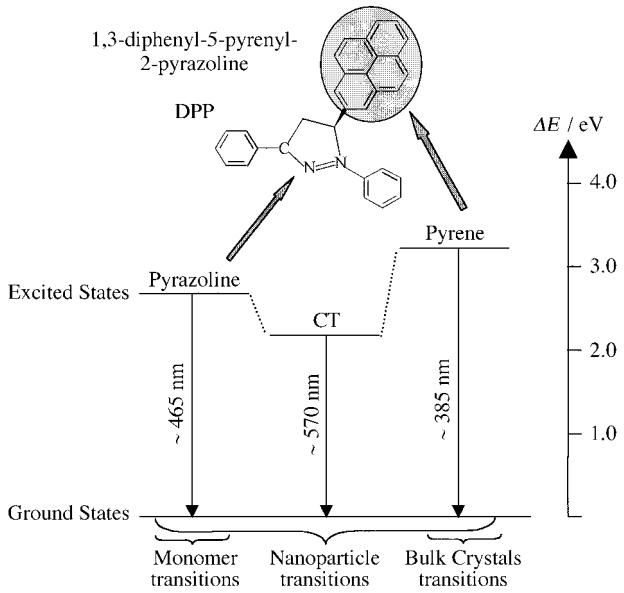

Figure 4. The emission transitions for DPP in monomers, nanoparticles, and bulk crystals.

characteristics of DP in ethanol solution, the nanoparticle emission at 465 nm is attributed to the pyrazoline group. It must be noted that the band at 400 nm in the corresponding excitation spectra (yellow lines) is not observed in the excitation spectrum of DP in ethanol solution, monitored at 460 nm. Whereas, for the PDDP nanoparticles[10] this band as well as that at 370 nm can be assigned to the charge-transfer

Table 1. The fluorescence decay times of different samples at room temperature.

Sample	Excitation wavelength [nm]	Monitored wavelength [nm]	Decay times [ns]
DPP nanoparticles	345	385	38.2 ± 0.42
		465	3.76 ± 0.30
		560	9.20 ± 0.33
DP in ethanol solution	360	460	4.23 ± 0.30
pyrene crystal[a]	345	395	–, 8[b]
		465	70, 180[b]

[a] From reference [13]. [b] Measured at 77 K.

state between pyrazoline groups and the pyrazoline ring π–π^* transition. The nanoparticle emission at 465 nm originates from aggregate states, which explains why the emission is not quenched by water. In contrast, the emission from the pyrazoline ring, caused by the twisted intramolecular charge transfer from the N-1 atom to the C-3 atom in the DPP in acetonitrile solution, is quenched by acetonitrile.[14, 15] The third band of the emission is unlikely to originate from the pyrene excimer, in which the emission wavelength is at 465 nm and the fluorescence lifetime is 70 ns at 298 K in pyrene crystals.[16] It can be seen that the excitation spectrum (Figure 3) corresponding to the third emission band (blue line) is similar to the corresponding absorption spectrum for each nanoparticle (NP1–NP4) shown in Figure 2, and includes the energy levels of both pyrene and pyrazoline groups. Therefore, we assigned it to an aggregated state of a charge-transfer complex between pyrene and pyrazoline groups. The broad features of the excitation spectrum are also indicative of a CT state.[17] Moreover, the gradually appearing feature at 450 nm in the absorption or excitation spectra (blue line in Figure 3), with increasing nanoparticle size, may originate directly from the energy level of the pyrene–pyrazoline CT states, since the 570 nm emission was observed by excitation using 450 nm light. The three nanoparticle emission bands at 385, 465, and 570 nm originate from the pyrene and pyrazoline groups and from a CT complex between the pyrene and pyrazoline groups, respectively.

The evolution of the multiple emissions of DPP nanoparticles is also studied as a function of nanoparticle size (Figure 3B–E). Compared with the spectra of the monomers shown in Figure 3A, molecular aggregation effects begin to influence the properties of DPP molecules in NP1. The greater intensity of the pyrene emission in Figure 3B than in Figure 3C–E indicates that individual molecules also play an important role in the properties of nanoparticles of this size, as do molecular aggregates. As the nanoparticle size increases, the emission at 570 nm is strongest in Figure 3c and then gradually decreases from Figure 3c to 3e. The orientation of the building units is identical because atoms can be regarded as hard spheres. However, the spatial configuration of organic molecules in organic nanoparticles plays an important role in their resulting properties. For example, the formation of intermolecular charge-transfer complexes demands that the donor–acceptor pair is in an approximately face-to-face arrangement, to give the largest orbital overlap.[4] Initially, when DPP molecules aggregate to form nanoparticles, two kinds of molecular aggregation, pyrazoline–pyrazoline

  1433-7851/02/4106-0964 $ 17.50+.50/0

(Py–Py) and pyrene–pyrazoline (Pr–Py) pairs, randomly begin to form nanoparticles such as those in NP1, which cause the emissions from them to overlap to some extent (Figure 3). As DPP nanoparticles grow further, as is the case for NP2(>100 nm), the enhanced Coulombic interaction energies between molecules[5] cause the Pr–Py pairs to form mainly on the surface of the nanoparticles, because of the larger volume of Pr–Py than Py–Py. This hypothesis explains why the emission from Pr–Py CT states at 570 nm is most intense in NP2 and then gradually decreases from NP2 to NP4(Figure 3); as a result of the decrease of the surface-to-volume ratio from NP2 to NP4. When the nanoparticle size increases further into the bulk phase, the Py–Py pair plays a dominant role in the properties of bulk crystals, and only pyrazoline-like emission is observed. The absence of pyrene monomeric emission in DPP bulk crystals may be a result of a low fluorescence quantum yield in bulk crystals as exhibited by the pyrene bulk crystals (as shown in Figure 3).[16] Therefore, the multiple emission of DPP nanoparticles and their evolution as a function of size is caused by the molecular aggregation and surface effects.

In summary, unlike the corresponding monomers and bulk crystals, DPP nanoparticles were found to exhibit a special type of multiple emission, which ranges from near-UV to green, and as a result of the surface effects, is tunable by alteration of both the excitation wavelength and nanoparticle size,. This novel phenomenon is of interest in the tailoring of the properties of optical materials. Thus, organic crystals also possess significant size effects like those of inorganic semiconductors and metals, but with a greater diversity because of a wide variety of organic molecular structures.

Received: August 27, 2001
Revised: October 22, 2001 [Z17800]

[1] M. A. Hinse, P. Guyot-Sionnest, *J. Phys. Chem.* **1996**, *100*, 468.
[2] A. P. Alivisatos, *Science* **1996**, *271*, 933.
[3] E. A. Silinsh, *Organic Molecular Crystals: Their Electronic States*, Springer, Berlin, **1980**.
[4] M. Pope, C. E. Swenberg, *Electronic Processes in Organic Crystals*, Oxford University Press, Oxford, **1982**.
[5] H. Kasai, H. Kamatani, S. Okada, H. Oikawa, H. Matsuda, H. Nakanishi, *Jpn. J. Appl. Phys. Part 2* **1996**, *35*(2B), L221.
[6] H. Kasai, H. Kamatani, Y. Yoshikawa, S. Okada, H. Oikawa, A. Watanabe, O. Itoh, H. Nakanishi, *Chem. Lett.* **1997**, 1181.
[7] H. Nakanishi, H. Katagi, *Supramol. Sci.* **1998**, *5*, 289.
[8] A. Ibanez, S. Maximov, A. Guiu, C. Chaillout, P. L. Baldeck, *Adv. Mater.* **1998**, *10*, 1540.
[9] Y. Z. Shen, D. Jakubczyk, F. M. Xu, J. Swiatkiewicz, P. N. Prasad, B. A. Reinhardt, *Appl. Phys. Lett.* **2000**, *76*, 1.
[10] H. B. Fu, J. N. Yao, *J. Am. Chem. Soc.* **2001**, *123*, 1434.
[11] X. C. Gao, H. Cao, L. Q. Zhang, B. W. Zhang, Y. Cao, C. H. Huang, *J. Mater. Chem.* **1999**, *9*, 1077.
[12] The size distribution of nanoparticles <100 nm is broad. For example, the polydispersity of nanoparticle NP1 of size 65 nm is about 40%.
[13] N. D. Denkov, O. D. Velev, P. A. Kralchevsky, I. B. Ivanov, H. Yoshimura, K. Nagayama, *Nature* **1993**, *361*, 26.
[14] J. O. Morley, V. J. Docherty, D. Pugh, *J. Mol. Electron.* **1989**, *5*, 117.
[15] Z. L. Yan, G. W. Hu, S. K. Wu, *Acta Chim. Sin. (Chinese Ed.)* **1995**, *53*, 227.
[16] A. Inoue, K. Yoshihara, T. Kasuya, S. Nagakura, *Bull. Chem. Soc. Jpn.* **1972**, *45*, 720.
[17] S. G. Schulman, *Fluorescence and Phosphorescence Spectroscopy: Physicochemical Principles and Practice*, Oxford, New York, **1977**.

Template Effects, Asymmetry, and Twinning in Helical Inclusion Compounds**

Mark D. Hollingsworth,* Michael E. Brown, Michael Dudley, Hua Chung, Matthew L. Peterson, and Andrew C. Hillier

Dedicated to Professor J. Michael McBride

Of the achiral substances in our world, only a small fraction are spontaneously resolved into enantiomorphic crystals that can be separated. Spontaneous resolution may occur when the molecular constituents of the crystal adopt chiral or skewed conformations or when molecules adopt chiral arrangements, such as a helices, which act as templates for further growth of the given enantiomorph. Certain inclusion compounds (such as those derived from urea and tri-*o*-thymotide) have received attention because spontaneous resolution of the inclusion compound leads to chiral discrimination between guest enantiomers.[1, 2] For urea inclusion compounds (UICs), in which urea forms helical channels in the presence of long-chain guests,[3] the literature has uniformly treated these materials as either right- or left-handed homochiral objects. In part, this misconception occurs because the typical needle morphology makes it difficult to observe the presence of enantiomorphic domains. Through the combined use of optical microscopy, synchrotron white beam X-ray topography (SWBXT), and crystallography, we demonstrate here the existence of two types of previously unrecognized macroscopic twinning in UICs. This work provides further support for our models of crystal growth[4] and hydrogen-bond topologies in UICs containing bis(methyl ketone)s[5] and provides a rationale for chiral (Brasil) twinning in these materials. This rationale may serve as a model for chiral twinning in other helical materials,[6] especially those with double helices.

Most urea inclusion compounds consist of well-defined host structures in which urea molecules are hydrogen-bonded to form honeycomb networks of nonintersecting hexagonal channels. Within these channels, long-chain guest molecules

[*] Prof. M. D. Hollingsworth, M. E. Brown, Dr. M. L. Peterson
Chemistry Department
Kansas State University
111 Willard Hall, Manhattan, KS 66506 (USA)
Fax: (+1) 785-532-6666
E-mail: mdholl@ksu.edu
Prof. M. Dudley, Dr. H. Chung
Department of Materials Science and Engineering
State University of New York at Stony Brook
Stony Brook, NY 11794 (USA)
Prof. A. C. Hillier
Department of Chemical Engineering
University of Virginia
Charlottesville, VA 22904 (USA)

[**] We thank J. D. Chaney, S. R. Wilson, B. D. Santarsiero, and J. M. McBride for help with this work, and the donors of the Petroleum Research Fund, administered by the American Chemical Society (29932-AC4), the NSF (CHE-0096157 and DMR-9996243), NASA (NAG8-1702), and the Research Corporation for funding. Topography was carried out at the Stony Brook Synchrotron Topography Station, Beamline X-19C at the National Synchrotron Light Source, Brookhaven National Laboratory, which is supported by the U.S. Department of Energy under contract number DE-AC02-98CH10886.

  1433-7851/02/4106-0965 $ 17.50+.50/0